Design and Implementation of 4S-Van: A Mobile Mapping System

Seung-Yong Lee, Kyoung-Ho Choi, In-Hak Joo, Seong-Ik Cho, and Jong-Hyun Park

Recent advances in positioning and photogrammetry technologies have made it possible to build a mobile mapping system (MMS) that can obtain 3D coordinates of geographic objects from stereo images recorded from a moving vehicle. In this paper, we present a design and detailed implementation of an MMS called a 4S-Van. Furthermore, we present four issues that have made major contributions to the performance of an MMS: 1) CCD camera calibration, 2) GPS signal condition, 3) integrating a GPS, inertial navigation system (INS), distance measurement indicator (DMI), and CCD cameras, and 4) the orientation angle of CCD cameras. In the experimental results, the performance of an MMS was analyzed for each component, giving an idea of how to effectively design and integrate each component in developing an MMS to get a maximal accuracy of 3D coordinates.

Keywords: MMS, 4S-Van, GPS, INS, CCD camera.

I. Introduction

Recently, telematics has received increasing interest as an emerging technology that aims at more efficient and safer driving. Telematics is a service integrated with various technologies such as telecommunication, positioning, mobile computing, voice recognition, and so on. Many telematics services are now being operated or have been planned to be launched. Among such services, the one most widely-used is a car navigation system (CNS), which is spotlighted as a leading service in telematics. Therefore, geospatial data (more specifically, a navigation map) is the most important item in telematics because accurate geospatial data is a necessary and essential part for providing navigation services to users [1]. A Geospatial database usually has a large volume and requires frequent updates, so an efficient construction and updating method is an important issue for various telematics and location-based services. Geospatial data have been constructed by digitizing aerial photos or vectorizing scanned paper maps. However, such methods cannot provide accurate data for generating a navigation map (digital map), or small objects along a road such as road signs and traffic lights that are very important information for car navigation services. A land survey with a GPS and total station can acquire details of urban facilities that cannot be obtained by aerial photography, but this requires much acquisition time and cost [2], [3].

To solve such problems concerning constructing a geospatial database, mobile mapping systems (MMSs) have been introduced and developed. An MMS is a platform (usually a vehicle) equipped with navigation and image sensors, and can acquire 3D coordinates of roads and roadside facilities. It can obtain accurate 3D coordinates of small objects that aerial photographing systems cannot acquire. Because of its great

Manuscript received July 20, 2005; revised Jan. 23, 2006.

Seung-Yong Lee (phone: + 82 42 860 1693, email: lsy9892@etri.re.kr), In-Hak Joo (email: ihjoo@etri.re.kr), Seong-Ik Cho (email: sicho@etri.re.kr), and Jong-Hyun Park (email: pjh@etri.re.kr) are with Telematics & USN Research Division, ETRI, Daejeon, Korea.

Kyoung-Ho Choi (email: khchoi@mokpo.ac.kr) is with Department of Electronic Engineering, Mokpo National University, Jeollanam-do, Korea.

mobility, it can rapidly construct and update geospatial data including a digital map and roadside facilities, thus it can be used as an efficient management tool for them [4], [5]. The early form of an MMS was a mobile highway inventory system (MHIS). It used a gyro, accelerometer, and odometer to determine the vehicle's position, and used a video camera to record objects around highways. Due to the limited accuracy of 3D coordinates, the system provides only approximated coordinates of objects around highways together with their visual record [6], [7]. To improve 3D positioning accuracy, Alberta MHIS of Canada introduced new positioning and orientation algorithms by adopting DGPS (differential global positioning system). This system provided the location of a moving vehicle (at a speed of 50 to 70 km/h) within an accuracy of 0.2 to 0.3 m [8]. Recently, various MMSs combining positioning technologies with photogrammetry have been reported. They have the capability to obtain 3D coordinates of geographic objects with higher accuracy [9], [10].

In this paper, we present the design and implementation of a mobile mapping system, called a 4S-Van, developed by our previous research [10]-[13], for creating and updating a digital road map for CNS effectively. Furthermore, we present an error analysis scheme to show how system performance can be affected by each implementation step. In this paper, we consider four key factors that have a major contribution to the performance of an MMS. The first one is camera calibration, which is the most basic and necessary step to build an MMS. We have built 2D and 3D targets to solve the problem, showing that a 3D target provides the better performance. Second, we have tested the relationship between GPS geometry and 3D coordinate accuracy. We provide the range of position dilution of precision (PDOP) for the optimal performance of an MMS. Third, we have tested a sensor integration method, which is the most important step to build an MMS. The Kalman filter and a smoothing filter have been implemented for sensor integration. The last one is an orientation angle of CCD cameras. We provide how the system performance is affected by changing the position and orientation parameters of cameras. The organization of this paper is as follows. In section II, the architecture of the 4S-Van and its hardware and software issues are explained. In section III, our implementation and error analysis scheme are presented. Also, various algorithms for implementing each step and their performance comparison will be provided. Finally, conclusions and future work are given in section IV.

II. 4S-Van System Description

The 4S-Van has been developed as an MMS to construct 3D coordinates of geographic objects, making it possible to build and update geospatial data or a navigation map for CNS. The 4S-Van is a moving vehicle equipped with image sensors (stereo CCD and video cameras) and navigation sensors (GPS, INS, and DMI). Figure 1 shows the hardware architecture of the 4S-Van, and Fig. 2 shows its physical sensor arrangement. The CCD cameras, GPS, and INS are installed on the roof of the vehicle, and an external synchronization device (ESD) is installed to synchronize the GPS data with the images captured by the CCD cameras. We installed two GPS receivers to acquire the heading and roll of the 4S-Van, and a DMI at the rear wheel of the vehicle to acquire its speed. Figure 3 shows the appearance of the 4S-Van.

With the synchronized sensor data, we acquire 3D coordinates

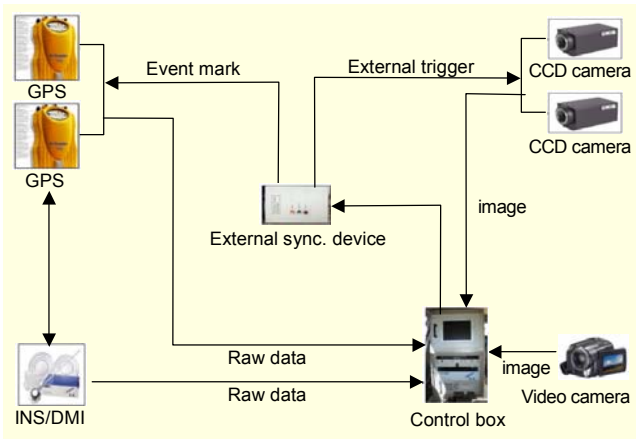

Fig. 1. The hardware architecture of the 4S-Van.

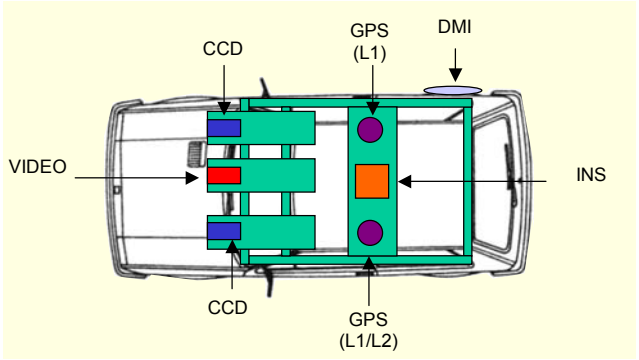

Fig. 2. The sensor arrangement of the 4S-Van.

Fig. 3. The appearance of the 4S-Van.

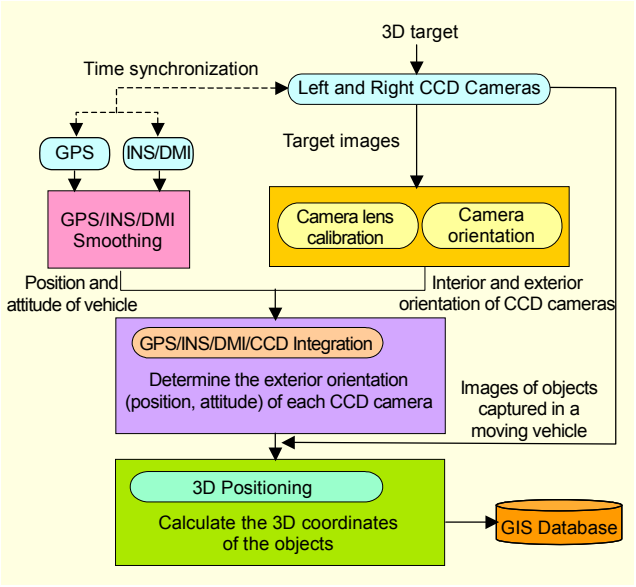

Fig. 4. The processing flow for calculating the 3D position of an object.

of objects through the following data processing steps: 1) A self-calibration for estimating the interior and exterior orientation parameters of CCD cameras; 2) GPS/INS/DMI integration for calculating the position and attitude of the vehicle; 3) CCD and GPS/INS/DMI integration for transformation between image coordinates in a camera frame and mapping frame using GPS/INS/DMI and CCD exterior orientation; and 4) 3D positioning of objects appearing in images for updating and creating the digital map. Figure 4 illustrates a data processing flow for calculating the 3D positions of objects by the 4S-Van.

1. Self-calibration

Generally, high-cost cameras designed for precise surveying, such as an aerial photo camera or land survey camera, specify parameters on focal length, principle point, and lens distortion [14]. However, when low-cost cameras are used, we must calculate the parameters by using a camera calibration algorithm periodically because the parameters are not known. In the case of the 4S-Van, a self-calibration method should be applied because high-cost cameras are not used. A self-calibration is a process that obtains the lens distortion parameter of CCD cameras by a fundamental space intersection algorithm, and obtains an exterior orientation as well as focal length, principal point, and lens distortion parameters using a least square method. The self-calibration method for the cameras of the 4S-Van is represented by

$$(x-x_p)+dx_r+dx_t=-f\frac{R}{Q},$$

$$(y-y_p)+dy_r+dy_t+dy_a=-f\frac{S}{Q},$$

$$\Delta r=k_1r^3+k_2r^5+k_3r^7,$$

$$dx_r=(x-x_p)\frac{\Delta r}{r}=(x-x_p)(k_1r^2+k_2r^4+k_3r^6),$$

$$dy_r=(y-y_p)\frac{\Delta r}{r}=(y-y_p)(k_1r^2+k_2r^4+k_3r^6),$$

$$dx_t=p_1(r^2+2(x-x_p)^2)+2p_2(x-x_p)(y-y_p),\quad dx_a=0,$$

$$dy_t=p_2(r^2+2(y-y_p)^2)+2p_1(x-x_p)(y-y_p),$$

$$dy_a=a_1(x-x_p)+a_2(y-y_p), \tag{1}$$

where f is the focal length, k_1, k_2, and k_3 are radial distortions, x_p and y_p are the principle points, p_1 and p_2 are tangential distortions, and a_1 and a_2 are affinities. For more details, refer to [14].

2. GPS/INS/DMI Integration

GPS/INS/DMI integration is the most important technology of the 4S-Van. The INS provides high-rate position, velocity, and attitude data with good short-term stability, while a GPS provides position and velocity data with good long-term stability [15]-[18]. By integrating a GPS with an INS, an enhanced navigation system that provides highly accurate navigation information can be developed. To enhance the performance of the 4S-Van, we apply a loosely coupled method for the overall integration design and a smoothing method for the integration filter design. The smoothing method yields a higher accuracy than a filtering method such as a Kalman filter because it uses the total measured value for estimating the state variable [19]. The implementation of a smoother is divided by three parts: fixed point, fixed lag, and fixed interval. The 4S-Van corrects navigation errors with a fixed interval smoother, which consists of a forward filter and backward filter that work independently with each other. The smoother of the 4S-Van consists of a forward filter by an extended Kalman filter, and a backward filter by a linear Kalman filter. The following equations represent the forward filter by the extended Kalman filter.

system model :

$$\dot{x}(t)=f[x(t),\,t]+G(t)w(t),\ w(t)\sim N[0,\,Q(t)]$$

measurement model :

$$z(t_k)=h[x(t_k),\,t_k]+v(t_k),\ v(t_k)\sim N[0,R(t)]$$

initial condition :

$$x(0)\sim N[\hat{x}_0,\,P_0],\ E\{w(t)v^T(t_k)\}=0\quad\forall t,t_k$$

propagation : $t_k^+\le t\le t_k^-$

$$\dot{\hat{x}}(t\,|\,t_k)=f[x(t\,|\,t_k),\,t],\quad \hat{x}(t_k\,|\,t_k)=\hat{x}(t_k^+)$$

$$\dot{P}(t\,|\,t_k)=F[t;\hat{x}(t\,|\,t_k)]P(t)+P(t)F^T[t;\hat{x}(t\,|\,t_k)]+G(t)Q(t)G^T(t)$$

update : $t = t_k^+$

$$\hat{x}(t_k^+) = \hat{x}(t_k^-) + K_k[z(t_k) - h[x_n(t_k),\, t_k] - H[t_k; x_n(t_k)]\{\hat{x}(t_k^-) - x_n(t_k)\}]$$

$$K_k = P(t_k^-)H^T[x_n(t_k),\, t_k] \cdot \{H[t_k; x_n(t_k)]P(t_k^-)H^T[t_k; x_n(t_k)] + R(t_k)\}^{-1}$$

$$P(t_k^+) = \{I - K_k H[t_k; x_n(t_k)]\}P(t_k^-)\{I - K_k H[t_k; x_n(t_k)]\}^T + K_k R(t_k) K_k^T \quad (2)$$

In (2), $\hat{x}(t_k^-)$ is the state variable, $P(t_k^-)$ is the covariance matrix calculated by time propagation, $\hat{x}(t_k^+)$ is the state variable at time k, $P(t_k^+)$ is the covariance matrix updated by using the measurement at time k, and K_k is the gain matrix of the filter. The following equations represent the backward filter by the linear Kalman filter. We used an estimated value of the forward filter for linearization of an INS.

initial condition : $\delta\hat{y}_b(0) = 0,\ P_b^{-1}(0) = 0$

propagation :

$$\overline{\delta}\,\hat{y}_b(\tau) = \{\overline{F}^T(\tau) - P_b^{-1}(\tau)\overline{Q}(\tau)\}\delta\hat{y}_b(\tau)$$

$$\overline{P}_b^{-1}(\tau) = P_b^{-1}(\tau)\overline{F}(\tau) + \overline{F}^T(\tau)P_b^{-1}(\tau) - P_b^{-1}(\tau)\overline{Q}(\tau)P_b^{-1}(\tau)$$

update :

$$\delta\hat{y}(\tau_k^+) = P_b^{-1}(\tau_k^-)\delta\hat{x}_f(t_f - \tau_k^+) + \delta\hat{y}_b(\tau_k^-) - H(\tau_k)R^{-1}(\tau_k)\delta z(\tau_k)$$

$$P_b^{-1}(\tau_k^+) = P_b^{-1}(\tau_k^-) + H^T(\tau_k)R^{-1}(\tau_k)H(\tau_k) \quad (3)$$

After estimating $\delta\hat{y}_b(t)$ by (3), we have a smoothing algorithm that combines $\delta\hat{y}_b(t)$ with the estimated $\hat{x}_f(t)$ of the forward filter, defined as

$$\hat{x}_s(t_k) = \hat{x}_f(t_k^+) - P_s(t_k)\delta\hat{y}_b(t_k^-). \quad (4)$$

The smoothing algorithm (4) derived in this paper should store the results of the forward filter, $\hat{x}_f(t_k^+)$, but it is simple to implement because it uses the results of the backward filter, $\delta\hat{y}_b(t)$. Because two GPSs, an INS, and a DMI are installed in different locations, a sensor integration algorithm should consider the location difference between sensors. Such vector between two sensors is called a lever-arm parameter and is denoted by Δr^b, as shown in Fig. 5.

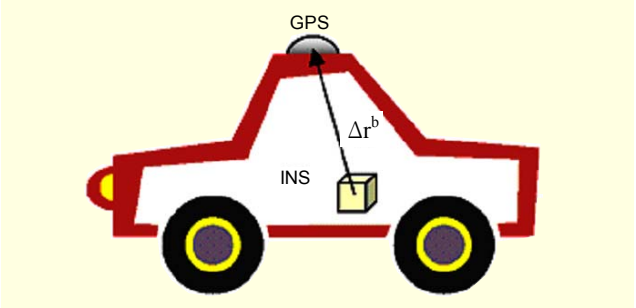

Fig. 5. Lever-arm parameter.

To consider the lever-arm parameter in the observed value of the Kalman filter, we process

$$r_{IMU}^n = r_{GPS}^n - \begin{bmatrix} \frac{1}{M+h} & 0 & 0 \\ 0 & \frac{1}{(N+h)\cos L} & 0 \\ 0 & 0 & -1 \end{bmatrix} C_b^n \Delta r^b \quad (5)$$

$$\delta r = \begin{bmatrix} \mathbf{I}_{3\times3} & \mathbf{0}_{3\times3} & \mathbf{I}_{3\times3} & \mathbf{0}_{3\times3} & \mathbf{0}_{3\times3} & \mathbf{0}_{3\times1} \end{bmatrix} \delta X + v, \quad (6)$$

where r_{IMU}^n is the position of INS by GPS measurement, r_{GPS}^n is the position measurement of the GPS, C_b^n is the attitude transformation matrix by using the navigation algorithm, and Δr^b is the weight parameter of the lever-arm vector. Refer to [16] for more details.

3. CCD/GPS/INS/DMI Integration

To get the 3D coordinates of objects from stereo images recorded from a moving vehicle, we must calculate the orientation (position and attitude) of each CCD camera. It can be estimated through a process that combines each camera's exterior orientation with the position and attitude of the vehicle using GPS/INS/DMI. That is, we obtain the exterior orientation of each CCD camera in a mapping frame by combining GPS/INS/DMI data in a navigation frame with its exterior orientation in an image frame. We carried out GPS/INS/DMI/CCD integration by using a bore-sight calibration algorithm because the navigation sensor and image sensor are installed in different locations. The bore-sight calibration algorithm [20] is represented by

$$\overline{X}_{NED}^{INS} = \begin{bmatrix} X_{INS} \\ Y_{INS} \\ Z_{INS} \end{bmatrix}_{NED} = \begin{bmatrix} X_{PC} \\ Y_{PC} \\ Z_{PC} \end{bmatrix}_{NED} + R_{BINS}^{NED} \begin{bmatrix} b_x \\ b_y \\ b_z \end{bmatrix} = \overline{X}_{NED}^{PC} + R_{BINS}^{NED} b_{INS},$$

$$S = \begin{bmatrix} 0 & 1 & 0 \\ 1 & 0 & 0 \\ 0 & 0 & -1 \end{bmatrix}, \quad R_{BINS}^{ENU} = SR_{BINS}^{NED}, \quad (7)$$

$$R_{Pht} = R_C^{ENU} = R_{BINS}^{ENU} R_C^{BINS}, \quad R_C^{BINS} = R^{T\,ENY}_{BINS} R_C^{ENU},$$

$$\delta\phi = \sin^{-1}(r_{13}), \quad \varphi\delta = \tan^{-1}\left(\frac{-r_{23}}{r_{33}}\right), \quad \varphi\kappa = \tan^{-1}\left(\frac{-r_{12}}{r_{13}}\right),$$

where R_{BINS}^{NED} is the rotation matrix offset defined in the INS body frame, $\overline{X}_{NED}^{INS}$ is the center coordinates of the INS in a navigation frame, $\overline{X}_{NED}^{PC}$ is the camera projection center coordinates in an NED navigation frame, and b_x, b_y, and b_z are the bore-sight offset in a body frame.

4. 3D Positioning

We carried out a space intersection method to calculate the 3D coordinates of an object by using the exterior orientation of each CCD camera (mapping frame) at exposure time, interior orientation by self-calibration, and stereo images of an object, as acquired from the 4S-Van in a moving environment. The space intersection algorithm [14] is represented by

$$
\begin{aligned}
&b_{14}dX_A + b_{15}dY_A + b_{16}dZ_A = J + v_{xa},\\
&b_{24}dX_A + b_{25}dY_A + b_{26}dZ_A = J + v_{xa},\\
&b_{14} = \frac{f}{q^2}(rm_{31} - qm_{11}), \quad b_{15} = \frac{f}{q^2}(rm_{32} - qm_{12}),\\
&b_{16} = \frac{f}{q^2}(rm_{33} - qm_{13}), \quad b_{24} = \frac{f}{q^2}(sm_{31} - qm_{21}),\\
&b_{25} = \frac{f}{q^2}(sm_{32} - qm_{22}), \quad b_{26} = \frac{f}{q^2}(sm_{33} - qm_{23}),\\
&J = x_a - x_o + f\frac{r}{q}, \quad K = y_a - y_o + f\frac{s}{q},
\end{aligned}
\tag{8}
$$

where f is the focal length, X_A, Y_A, Z_A are model coordinates, and m_{11} through m_{33} are elements of the rotation matrix.

III. Implementation and Error Analyses

In this section, the detailed implementations of four issues that have made major contributions to the performance of an MMS are described. The four issues are as follows: 1) CCD camera calibration; 2) GPS signal condition; 3) integrating a GPS, INS, DMI, and CCD cameras; and 4) orientation angle of CCD cameras. For each issue, we present our implementations and compare the performances. For the experiment, we use Litton's INS, LN-200, dual frequency Trimble GPS receivers, and two color CCD cameras. The INS has gyro biases of around 3 degrees per hour and accelerometer biases of around 300 μg. The CCDs have a resolution of 1392 by 1040 and a unit cell size of 4.65 μm by 4.65 μm. For the field test of the 4S-Van, we selected a test area and obtained trajectories that contain almost all the conditions needed for the performance evaluation of the 4S-Van, including a tree-lined road, tunnel, and urban area. We collected nine test trajectories, about 30 minutes long. Figure 6 shows the implemented program for each process of our experiments.

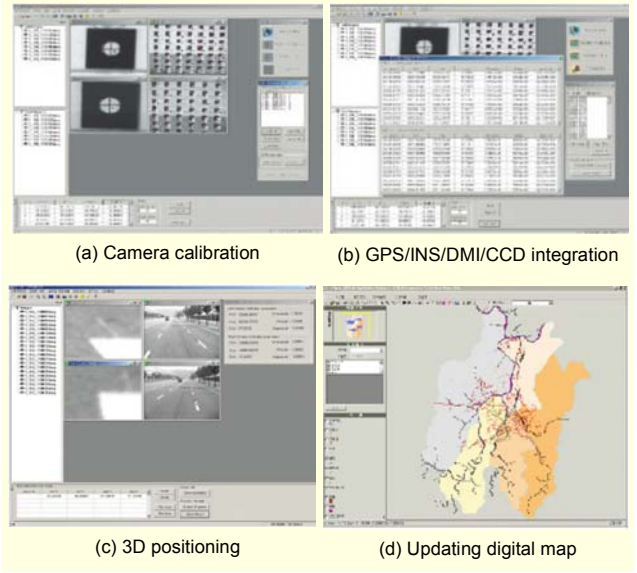

Fig. 6. Program for experiments.

1. CCD Camera Calibration

Calibration of a CCD camera is one of the most basic and important implementation steps for obtaining 3D coordinates of objects. In our implementation, a 3D target area is installed on the wall, as shown in Fig. 7, and the 3D accuracies of the systems, calibrated through each target, are compared. Table 1 shows the comparison of 3D accuracies for several targets. As indicated in Table 1, the performance of 3D positioning can be improved by using a 3D target. In the case of a plane 2D target, the focal length and principle point have high correlation with the projection center of the camera. We can reduce such correlation by using a 3D target. With such a 3D target used, we can correct the tangential distortion and affinity parameters that a conventional 2D target cannot correct, as well as the focal length, principle point, and radial distortion. The target area itself has 117 target cylinders over the wall with the dots located in the middle of the cylinders. To collect the calibration data, we captured the images of the target area at the front where all dots in the targets are clearly visible in the image. The detailed target settings are as follows:

- wall size for establishing target area: width = 2.30 m, length = 1.90 m
- total number of targets: 117 (81 are 2D and 36 are 3D.)
- 3D target sizes (height): 10 cm, 20 cm, 30 cm (12 each)

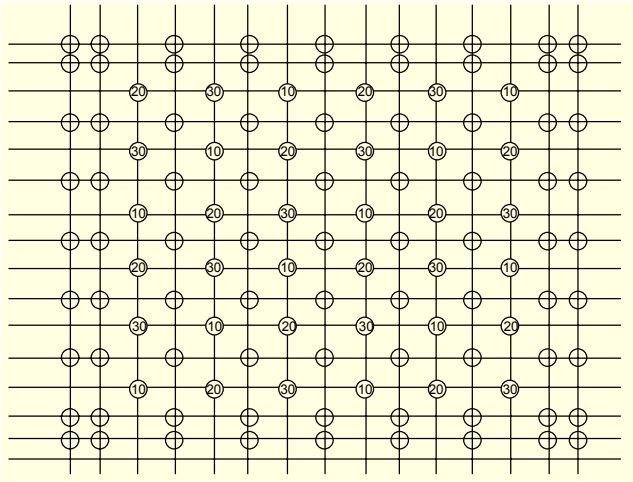

Fig. 7. The calibration of 3D targets.

Table 1. Comparison of positioning accuracy of the 3D targets.

ID	Method	X (m)	Y (m)	Z (m)	Error (m)
1	GPS survey	234258.6	317742.6	43.045	
	2D target	234258.7	317742.5	43.25	0.225765
	3D target	234258.6	317742.5	43.23	0.199374
2	GPS survey	234250.6	317742.5	43.082	
	2D target	234250.7	317742.6	43.28	0.215539
	3D target	234250.5	317742.6	43.26	0.187235
3	GPS survey	234223.7	317746.1	43.054	
	2D target	234224.0	317746.1	43.19	0.348276
	3D target	234223.8	317746.1	43.14	0.110887

2. GPS Signal Condition

Unlike the cases of an aerial photographing survey, an MMS does not use ground control points. Instead, GPS and INS data are used to decide the current coordinate and attitude information of the vehicle, which means data quality from the two sensors is most important for the performance of an MMS. Because GPS data are acquired as the vehicle is moving, the receiving condition of a GPS signal varies from time to time according to the surrounding objects such as buildings, trees, and terrain, which have important effects on the accuracy of 3D positioning of objects. To analyze the relationships between GPS geometry and accuracy of 3D coordinates of an object, we check the position errors of objects with regard to changing GPS satellite numbers received in the same area. Table 2 shows the difference between 3D coordinates of a chosen point calculated by the 4S-Van and its actual coordinates surveyed by the total station in advance, with regard to changing visible satellite numbers. As the number of visible satellites increases, PDOP and overall errors are decreased, as shown in Table 2.

Table 2. Position errors with regard to various numbers of satellites.

No. of satellite	PDOP	GPS (m)			Average position errors of objects calculated by 4S-Van		
		SD_X	SD_Y	SD_Z	D_X	D_Y	Error
7	1.9	0.024	0.020	0.033	0.125	0.097	0.198
6	1.71	0.024	0.017	0.042	0.127	0.091	0.181
5	1.98	0.022	0.022	0.050	0.288	0.267	0.576
4	2.26	0.081	0.094	0.067	0.537	0.694	1.347

Positional accuracy is excellent if the PDOP value is under 2, however, when the PDOP value is over 6, the data have too large of errors to calculate 3D coordinates. Thus, we need to process in an adequate time interval to increase the accuracy of 3D coordinates by analyzing the PDOP and number of visible satellites beforehand.

3. Integrating Sensors

The most important step in developing an MMS is integrating positioning sensors, for example, a GPS, INS, and DMI. We have implemented a Kalman filter and a smoother (please refer section II.2 for details). In our implementation, we used positional data calculated from a CDGPS (Carrier DGPS) for a reference trajectory. Figure 8 shows the position determined by the smoother and Kalman filter. The smoother shows better performance than the Kalman filter. This is because the smoother uses measurements before and after a certain time for estimating the state variable, while the Kalman filter does not use future time measurements. Integrating a DMI can also help

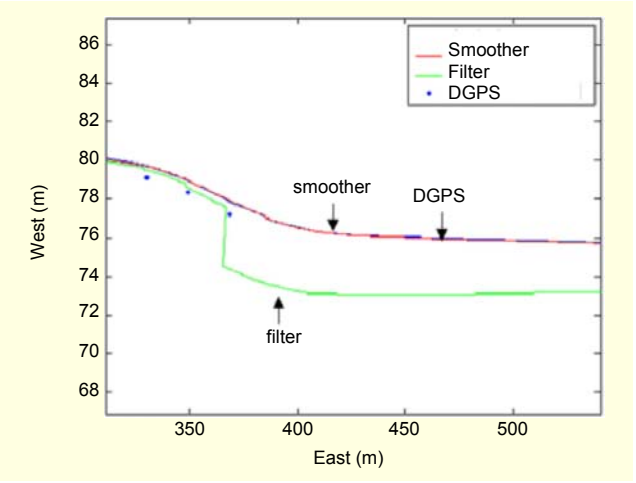

Fig. 8. Smoother vs. filter.

in enhancing navigation accuracy when a GPS signal is interrupted over a long period of time, as shown in Fig. 9. The change of error covariance of the forward filter is shown in Fig. 10,

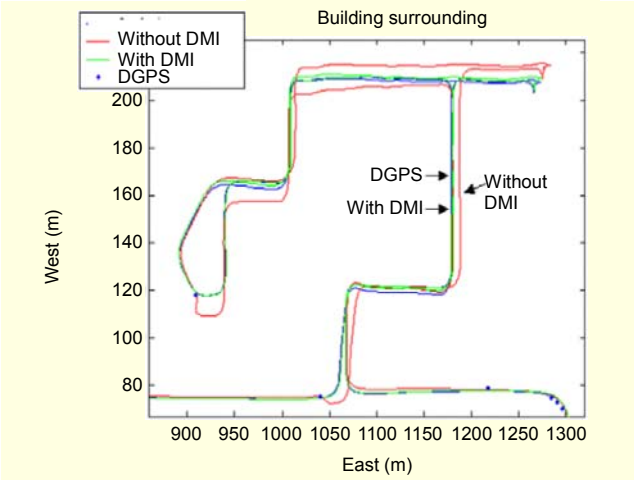

Fig. 9. With vs. without DMI.

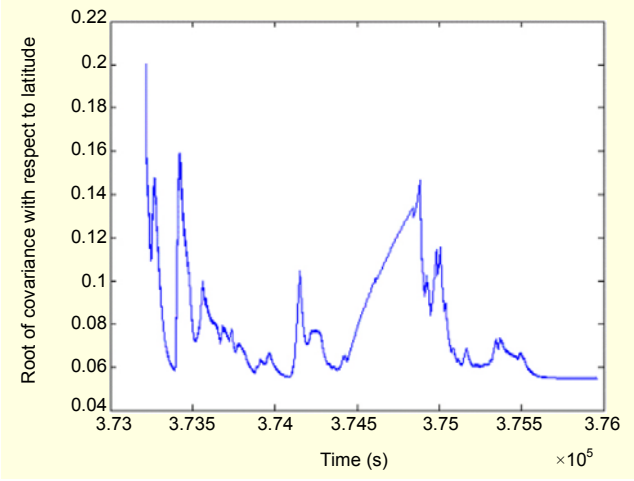

Fig. 10. Forward filter covariance.

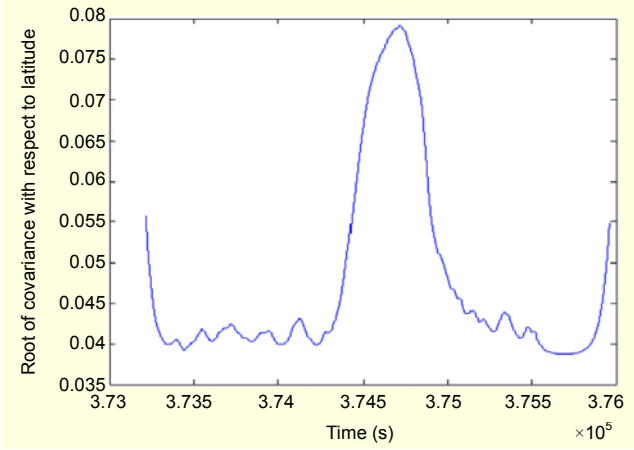

Fig. 11. Smoother covariance.

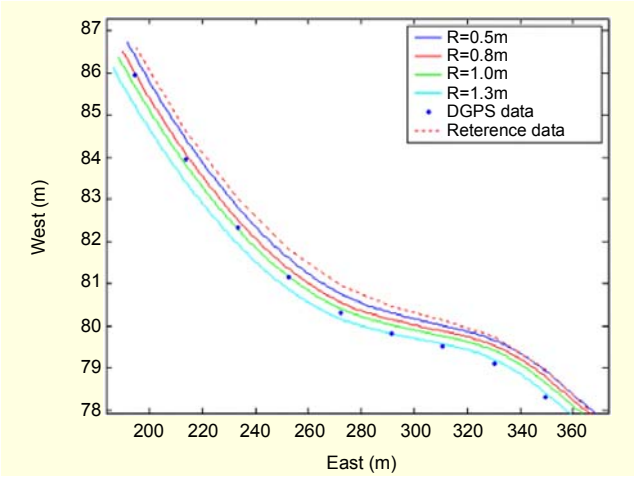

Fig. 12. Covariance tuning of DGPS measurement.

while the change of error covariance of the smoother is shown in Fig. 11. Figure 12 shows an improvement in accuracy by adjusting the covariance of the measurement noise.

In conclusion, assuming that the navigation solution is calculated by post-processing, the smoothing method shows better performance of reducing navigation errors compared with the Kalman filter.

4. Orientation Angle of CCD Cameras

Photogrammetry is a method that extracts 3D coordinates of an object by using the exterior orientation (position and attitude) of stereo cameras. The accuracy of 3D coordinates is inversely proportional to the distance between cameras and objects. Various geographic objects such as traffic signs and street lights were chosen to check the accuracy of 3D coordinates for different distances between cameras and the chosen objects, as shown in Fig. 13.

As shown in Table 3, because of the difficulty in finding accurate matching points in stereo images, 3D errors become large when the distance between cameras and objects is long. In addition to the distance between cameras and objects, the angle of the cameras also has to be determined carefully. We should adjust the angle of CCD cameras depending on the objects to measure. Figure 14 shows four cases of camera angles used for our experiments, and Fig. 15 shows an example

Fig. 13. The observed road borders with regard to changing distance.

Table 3. Position error with regard to changing distance.

Object	Position of camera			Distance	3D position			Error
	X	Y	Z		X	Y	Z	
Traffic sign	231323.38	321435.07	58.24	24.38	231340.62	321453.16	57.49	0.61
	231326.45	321439.18	58.01	19.29	231340.42	321452.90	57.20	0.29
	231329.72	321443.75	57.77	13.80	231340.44	321452.77	56.74	0.23
Street light	231329.72	321443.75	57.77	22.24	231346.06	321459.54	56.77	0.49
	231332.50	321447.58	57.58	17.60	231346.02	321459.45	56.33	0.40
	231335.16	321451.13	57.42	13.29	231345.85	321459.25	55.99	0.14
Road border	232187.88	320544.58	53.34	20.66	232168.07	320551.43	50.68	0.45
	232182.27	320545.73	53.12	14.99	232168.28	320551.31	50.72	0.29
	232176.43	320546.92	52.89	9.15	232168.36	320551.23	50.76	0.24

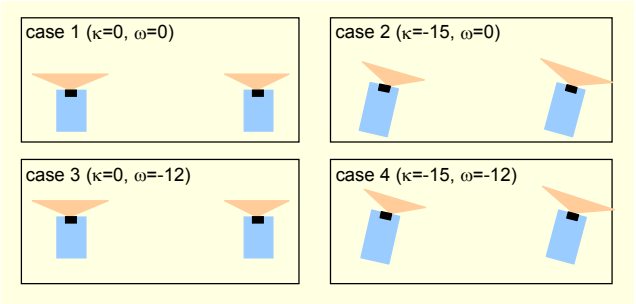

Fig. 14. Cases of camera angle.

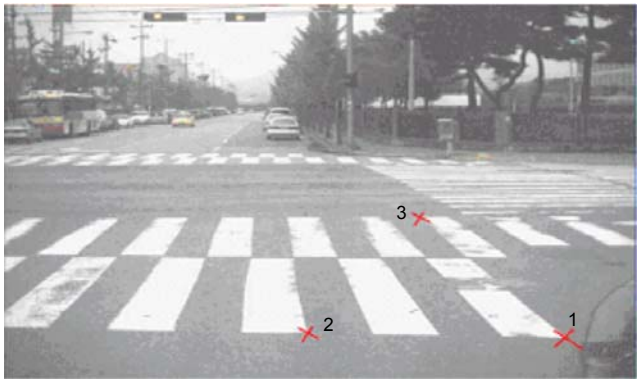

Fig. 15. An example of chosen points.

Table 4. Comparison of accuracy for each case.

Test	Error			
	ΔX (m)	ΔY (m)	ΔZ (m)	RMSE
Case 1	-0.69	-0.14	0.20	0.73
Case 2	-0.75	-0.19	0.20	0.80
Case 3	-0.09	-0.29	0.12	0.32
Case 4	-0.10	-0.35	0.15	0.39

image in which several points are observed.

When we adjust the camera angle as in case 1 or case 2, about a 0.7 to 0.8 m error occurs because the distance between object and camera is long. Although the accuracy is worse than in case 3 and case 4, case 1 and case 2 have the advantage of obtaining objects in a wide area. The accuracy of case 3 and case 4 are higher than case 1 and case 2, assuming that roads and roadside facilities are the main objects to measure. In conclusion, to improve accuracy of the 4S-Van, we should adjust the camera angle case by case according to the kind of objects whose coordinates will be acquired.

IV. Conclusion

In this paper, we have presented the implementation of an

MMS called a 4S-Van, which was designed to obtain 3D coordinates of objects along a road. We also have discussed the performance of the 4S-Van, evaluating the performance through an error analysis for each implementation step. We have discussed four issues that make major contributions to the performance of the 4S-Van, which are summarized as follows:

1) For camera calibration, a 3D target is better than a plain 2D target for system performance because it can remove the high correlation of focal length and principle point with the projection center of a camera.
2) Because the performance of GPS/INS integration depends on the data quality of a GPS signal, we need to increase the accuracy of 3D coordinates in poor conditions after sufficiently receiving the GPS signal in a good signal condition environment.
3) For integrating a GPS, INS, and DMI, the suggested smoother shows better performance than the Kalman filter due to its characteristic of considering future measurements in the case of obtaining a navigation solution by post-processing.
4) Because the accuracy of 3D coordinates is inversely proportional to the distance between cameras and objects, the orientation angle of CCD cameras has to be determined according to the kind of objects.

Besides, it is obvious that the scale factor becomes larger when the velocity rapidly changes (for example, a turn at an intersection), assuming a low-cost INS is not stable and robust. Thus, a calibration such as zero velocity update should be done when the INS yields relatively large errors.

In summary, according to results of performance analyses, we conclude that we can enhance the accuracy of 3D coordinates calculated by the 4S-Van by considering and implementing the four issues just discussed.

Reference

[1] Chatschik Bisdikian, "Intelligent Pervasive Middleware for Context-Based and Localized Telematics Services," *Proc. of the 2nd International Workshop on Mobile Commerce,* ACM Press, 2002, pp. 15-24.

[2] N. El-sheimy, "The Development of VISAT–A Mobile Survey System for GIS Applications," *UCGE Report*, Department of Geomatics Engineering, University of Calgary, no. 20101, 1996.

[3] C.M. Ellum and N. El-sheimy, "Land-Based Integrated Systems for Mapping and GIS Applications," *Survey Review,* vol. 36, no. 283, 2002, pp.323-339.

[4] R. Li, "Mobile Mapping - An Emerging Technology for Spatial Data Acquisition," *Journal of Photogrammetric Engineering and Remote Sensing,* vol. 63, no.9, 1997, pp.1085-1092.

[5] N. El-sheimy, K.P. Schwarz, "Kinematic Positioning in Three Dimension Using CCD Technology," *Conf. of VNIS1993*, Oct. 1993, pp. 472-475.

[6] K.P. Schwarz, "INS/GPS as a Georeferencing Tool for Multi-Sensor Systems," *Mobile Mapping Symposium*, Columbus, OH, May 1995.

[7] Pierre-Yves Gillion, "Development of a Low Cost Mobile Mapping System for Road Database Management," *3rd International Symposium on Mobile Mapping Technology,* Jan. 2001, pp. 1-12.

[8] K.P. Schwarz, H.E. Martell, El-Sheimy, R. Li, "VISAT-A Mobile Highway Survey System of High Accuracy," *Conf. of VNIS 1993,* Oct. 1993, pp. 476-481.

[9] C. Tao, R. Li and M.A. Chapman, "A Model Driven Approach for Extraction of Road Line Features Using Stereo Image Sequences from a Mobile Mapping System," *Proc. of ASPRS/ACSM,* 1996.

[10] ETRI, *Annual Report on Development of Integration Technology for Spatial Information Systems*, 2002, pp. 249-302.

[11] GPSVan project, http://www.cfm.ohio-state.edu

[12] GPSVision project, http://www.lambdatech.com

[13] Transmap project, http://www.transmap.com

[14] Paul R. Wolf, Bon A. Dewitt, 3rd ed., *Elements of Photogrammetry with Application in GIS*, McGraw-Hill, 2000.

[15] Elliott D. Kaplan, *Understanding GPS: Principles and Applications,* Artech House, 1996.

[16] D. H. Titterton and J. L. Weston, *Strapdown Inertial Navigation Technology,* Peter Peregrinus Ltd., 1997.

[17] R. B. Miller, "A New Strapdown Attitude Algorithm," *J. Guidance*, vol. 6, no. 4, 1983, pp. 287-291.

[18] Seong-Baek Kim, Kyung-Ho Choi, Seung-Yong Lee, "A Bimodal Approach for Land Vehicle Localization," *ETRI Journal,* vol. 26, no. 5, Oct. 2004, pp. 497-500.

[19] R. G. Brown and P. Y. C. Hwang, *Introduction to Random Signals and Applied Kalman Filtering,* 3rd ed., John Wiley and Sons, New York, 1997.

[20] Jan Skaloud, "Problems in Direct-Georeferencing by INS/DPGS in the Airborne Environment," *ISPRS Workshop*, 1999, pp. 25-26.

Seung-Yong Lee received the BS and MS degrees in electronic engineering from Chungnam National University, Daejeon, Korea in 1999 and 2001. Since 2001, he has been working for Electronics and Telecommunications Research Institute

(ETRI) in Korea as a researcher. Currently he is a member of the Telematics and USN Research Division of ETRI. His research interests include global navigation satellite systems, location-based services, and telematics.

Kyoung-Ho Choi received the BS and MS degrees in electrical and electronics engineering from Inha University, Incheon, Korea, in 1989 and 1991. He received the PhD degree in electrical engineering from the University of Washington, Seattle in 2002. Beginning in January 1991, he was with ETRI, where he was a leader of the Telematics-Content-Research Team. He was also a visiting scholar at Cornell University, Ithaca, NY, in 1995. In March 2005, Dr. Choi joined the Department of Electronic Engineering of Mokpo National University, Jeonnam, Korea. His research interests include telematics, sensor networks, multimedia signal processing and systems, mobile computing, MPE4/7/21, and audio-to-visual conversion.

In-Hak Joo received the BS, MS, and PhD degrees in computer science from Yonsei University, Seoul, Korea, in 1992, 1994, and 2000. Since 2000, he has been working for ETRI in Korea as a Senior Researcher, where he is currently a member of the Telematics and USN Research Division. His research interests include geographic information systems, spatial databases, and telematics.

Seong-Ik Cho is a Research Team Leader in the Telematics and USN Research Division of ETRI. He received the BS and MS degrees from Yonsei University, Seoul, Korea, in 1984 and 1987. He worked on the Research Staff in Systems Engineering Research Institute from 1987 to 1996, and has been working for ETRI from 1996. His research interests are in remote sensing, computer vision, and telematics.

Jong-Hyun Park received the BS and MS degrees in the Departments of Space Science and Astronomy & Meteorology in KyungHee and Yonsei Universities, Seoul, Korea, in 1989 and 1991, respectively. He received the PhD degree in environmental engineering from Chiba University, Japan, in 2000. Since 1991, he has been with ETRI, where he is currently a Director of the Telematics Research Group. His research interests include location-based services, telematics, WSN (wireless sensor network) middleware, and positioning systems using a global navigation satellite system.